72255

Aphanitic Impact Melt Breccia
St. 2,461.2 g

INTRODUCTION

72255 is an aphanitic, clast-rich impact melt that was a rounded mass or bulge on Boulder 1 (see section on Boulder 1, St. 2, Fig. 2). It may have been part of a single large clast in the boulder (Marvin, 1975a). Its groundmass crystallized about 3.8 Ga ago. The sample, slightly more than 10 cm long but only 2.5 cm wide, is subrounded on all faces except for the freshly broken interior (Fig. 1). 72255 is moderately coherent, heterogeneous, and polymict, with color varying from medium light gray (N6] to light gray [N5]. The exposed surfaces show a firm dark patina with some zap pits (Fig. 2).

72255 is superficially similar to 72275, but is more coherent. It is fine-grained and heterogeneous, with prominent clasts and a zone rich in chalky white lenses and stringers. The most prominent class in Fig. 1 is the Civet Cat norite, a 2-cm cataclastic fragment with a relict plutonic texture and a probable crystallization age of 4.12 Ga. Other clasts include aphanitic melt blobs and fragments, anorthositic breccias, feldspathic granulites, basaltic/troctolitic impact melts, and granites. The melt groundmass has a low-K Fra Mauro composition similar to others in the boulder. Rare gas analyses show an exposure age of about 43 m.y.

Most of the studies of 72255 were conducted by the Consortium Indomitable (leader J.A. Wood). A

Figure 1: Top (arbitrary) face of 72255, the broken interior. The dashed lines show the location of the cuts for the slab. The prominent clast between the lines is the Civet Cat norite. The area to the right (east) is a zone rich in chalky white lenses and stringers. Scale in cm. S-73-23726B.

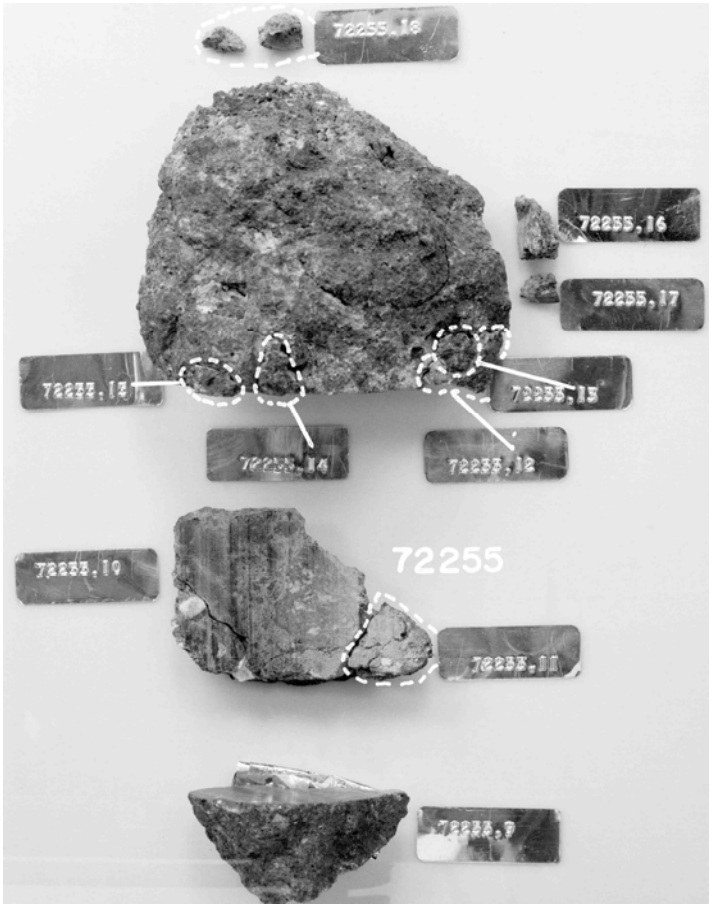

Figure 2: Slab cut from 72255 (center). Lower is west end, upper is main mass, showing exterior patina, and location of other chips. The slab was further dissected. Scale in cm. S-73-32620.

slab was cut across the sample to include the Civet Cat clast (Figs. 1, 2), providing samples for comprehensive petrographic, chemical, and isotopic studies. Detailed maps of the exterior surfaces and the slab based on macroscopic observations, as well as descriptions of the sample allocations, are in Marvin (in CI 1, 1974).

PETROGRAPHY

Specimen 72255 consists of coherent material that is dominantly a dark matrix breccia (Marvin, in Cl 1,1974; 1975a; Stoeser et al., in CI 1,1974; 1974a,b; Ryder et al., 1975b). Stoeser et al. (1974a) suggested about 60% matrix, although what constituted matrix was not clearly defined; it was described as "small monomineralic and lithic clasts in a finely recrystallized submatrix". The dark breccia material is polymict, with a groundmass that is a fine-grained impact melt (e.g. James, 1977; Spudis and Ryder, 1981). LSPET (1973) listed the sample as a layered light gray breccia. Simonds et al. (1974) described 72255 as a clast-supported fragmental breccia, with both matrix feldspars and matrix mafic minerals smaller than 5 microns, and some angular clasts larger than 30 microns. Knoll and Stoffler (1979) described 72255 as having a dark, fine-grained, equigranular crystalline matrix that contains some areas of lighter, coarser-grained matrix.

The thin sections show a melt groundmass similar to that of 72215 (Fig. 3a,b), polymict and dense. The fine material consists of abundant small monomineralic and lithic clasts in a crystalline melt groundmass that consists of plagioclase, pyroxene, and disseminated ilmenite tablets. Magnetic data show that the matrix has about 0.76% metallic iron (Banerjee and Swits, 1975). The monomineralic clasts are plagioclase, olivine, orthopyroxene, clinopyroxene, and sparse-to-trace pink-to-red spinel, chromite, and ilmenite. Compositions of the olivines and pyroxenes are shown in Fig. 4; at least most of the olivines are clasts, not melt-crystallized phases. The olivines include examples more forsteritic than those in the anorthositic and granulitic clasts. The only lithic fragments in the sample with such forsteritic olivine are the basaltic troctolites. The magnesian pyroxenes have no counterpart in any lithic fragments from the boulder. The mineral compositions in 72255 have compositional ranges similar to those in 72215 and the dark breccias in 72275. Ryder (1984a) analyzed olivine fragments in 72255, finding that many have calcium contents high enough (0.05-0.15%) to be consistent with having an origin in shallow, rather than deep, plutonics.

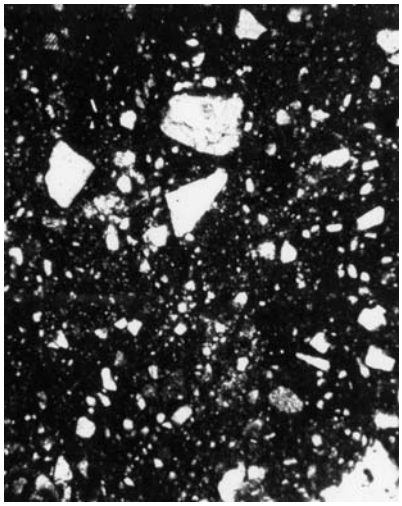

a

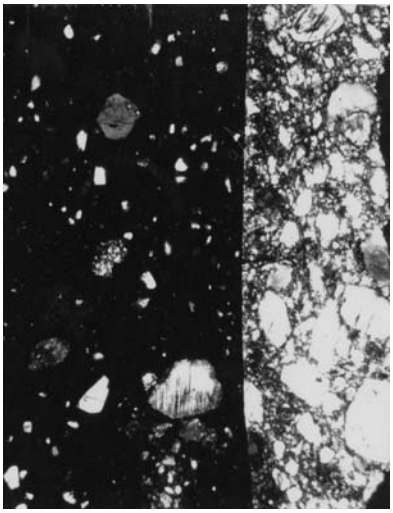

b

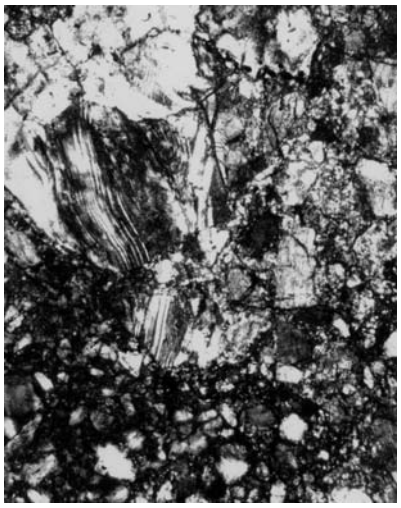

c

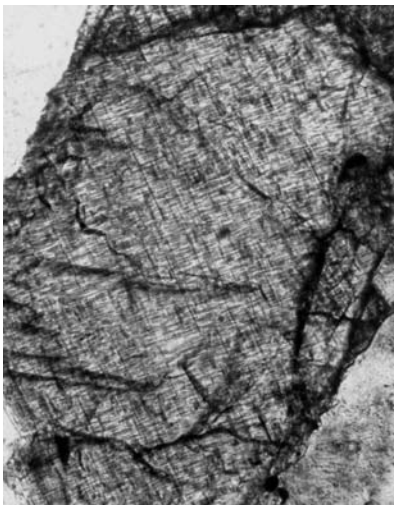

d

Figure 3: Photomicrographs of materials in 72255. Width offield about 1.5 mm, except for d) which is about 300 microns Figures a and d are crossed polarizers; b and c plane light.

a) 72255, 89; general matrix showing dense dark impact melt with angular to subrounded small mineral and lithic clasts.
b) 72255, 130; contact between Civet Cat norite (right) and groundmass (left). The contact is extremely sharp and straight, without evidence of reaction.
c) 72255, 123; Civet Cat write, with deformed plagioclase (top) and crushed orthopyroxene (bottom).
d) 72255, 123; orthopyroxene in Civet Cat norite, showing its lineated features.

Table 1: Defocused beam analyses of groundmass of 72255 (Stoeser *et al.*, in CI 1, 1974).

	3	4
	72255, 95 matrix	72255, 105 Civet Cat rind
SiO_2	45.1	46.5
TiO_2	0.6	0.9
Cr_2O_3	0.2	0.2
Al_2O_3	20.0	21.4
FeO	7.7	8.5
MnO	0.1	0.1
MgO	9.1	9.4
CaO	12.7	12.3
Na_2O	0.5	0.3
K_2O	0.2	0.2
P_2O_5	0.2	0.4
Total	96.4	100.2
Fo	4.3	1.9
Fa	2.8	1.2
En	17.3	20.8
Fs	10.2	12.1
Wo	4.3	0.8
Or	1.3	1.3
Ab	4.1	2.3
An	53.9	56.5
Ilm	1.1	1.7
Chr	0.2	0.3
Qtz	0.0	0.0
Cor	0.0	0.0
Ap	0.5	0.8

Table 2: Clast population survey of particles greater than 200 microns in diameter in 72255. Percent by number, not volume. (from Stoeser *et al.*, 1974a).

Clast type	72255
Granulitic ANT breccias	31.3%
Granulitic polygonal anorthosite	6.3
Crushed anorthosite	5.2
Devitrified glass	13.8
Glass shards	—
Ultramafic particles	1.5
Basaltic troctolite	2.2
Pigeonite basalt	—
Other basaltic particles	1.9
Granitic clasts	2.6
"Civet Cat" type norite	0.7
Monomineralic plagioclase	19.3
Monomineralic mafic silicates	14.5
Monomineralic spinel & opaques	0.7
Number of clasts surveyed	269

The chemical composition of the groundmass (including small clasts) derived by defocused beam microprobe methods is low-K Fra Mauro basalt (Table 1; see also chemistry section), similar to other samples from the boulder and differing from coarser Apollo 17 impact melts in its lower Ti02 and higher A1203. Goswami and Hutcheon (1975) using fission track methods found that U was uniformly distributed on a 10 micron scale. Some of the matrix areas are lighter-colored, and more feldspathic, and contain clasts of dark matrix breccia, visible on the sawn surfaces. In thin sections the dark clasts are difficult to distinguish from the groundmass, and evidently are of very similar material. Ile groundmass has reacted with the clasts, producing re-equilibration rims up to 15 microns thick around pyroxenes and olivines, and reaction rims around spinels and granite clasts. Some of the granites have partially-melted internally, and all the glasses are devitrified, including those of feldspar composition that were presumably once maskelynite. All these features demand a high temperature (more than 800 or 900 degrees C), but lack of total equilibration shows that the high temperatures were not maintained for long periods:

A wide variety of lithic clasts is present in 72255. The clast population (Table 2) is similar to that in 72275, but lacks the volcanic KREEPy pigeonite basatis. Other basaltic fragments are present. The dark gray melt clasts/blobs are abundant, but the anorthositic clasts are relatively small and rare. Most of the latter are pure white, sugary, and granulitic. The types of material are described in Stoeser et al. (in Cl 1, 1974; in CI 2, 1974; 1974a,b) and Ryder et al. (1975b), mainly without specific identification of those clasts from 72255 except for photomicrographs. The granites were described by Stoeser et al. (1975) and Ryder et al. (1975a). They include varieties with feldspars in the "forbidden" compositional field (ternary feldspars), about $An_{55}Or_{40}$ Defocused beam microprobe analyses of anorthositic breccias, troctolitic basalts, and devitrified glasses are given in Table 3; similarly-produced analyses for a basaltic particle and a granite are given in Table 4. The analysis of the Civet Cat norite in Table 4 is an estimate (see Table caption).

The Civet Cat clast that is conspicuous on the broken face of the sample (Fig.1, 2) is an angular fragment about 2.5 cm long with light lenses and streaks in a dark groundmass. The rock is a cataclastic norite, essentially bimineralic and with a grain size originally of 1 to 4 mm (Stoeser et al., 1974a; Ryder et al., 1975) Orthopyroxene and plagioclase (Figs. 3b, c, d) have very narrow compositional ranges (Fig. 5). The plagioclase ($An_{92-94}Or_{0.5-1.0}$) is partially transformed to maskelynite and otherwise deformed (Fig. 3c). The orthopyroxenes (En72-74Wo2-4) is commonly kinked, and contains abundant small brown plates of ilmenite along the cleavage planes. Rare augite is present as small grains and lamellae. Accessory minerals include cristobalite, baddeleyite, ilmenite, chromite,

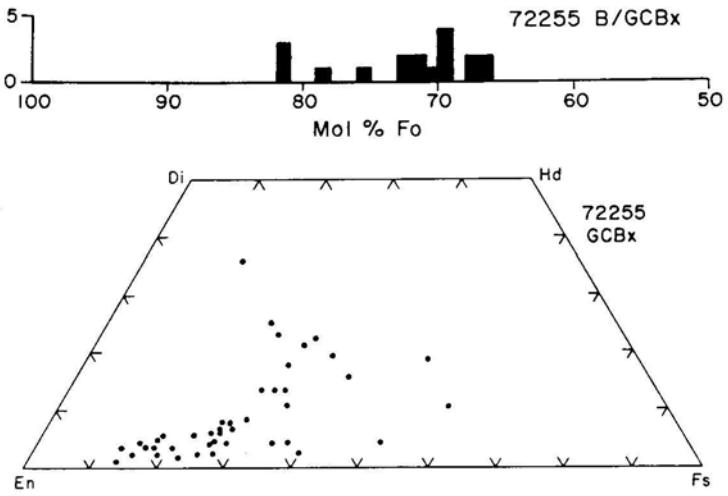

Figure 4: Compositions of monomineralic olivines and pyroxenes in groundmass of 72255 (from Ryder et al., 1975b).

Table 3: Defocused beam analyses of feldspathic granulitic clasts (cols. 14), anorthosite breccia (col. 5), polygonal anorthosite (col. 6), troctolitic clasts (cols. 7-9), and devitrifled glasses (cols. 10-12)
(from Stoeser *et al.*, in 011,1974; Ryder *el al.*, 1975b).

	2 770C7	3 770C12	4 770C24	5 770C27	6 770C26	7 770C37	770C2	770C30	770C77	1 770C10 devitrified glass	2 770C39 devitrified glass	3 770C83 devitrified maskylenite
SiO_2	43.9	46.2	51.1	44.3	44.9	42.8	42.3	42.5	41.2	44.0	42.4	44.8
TiO_2	0.1	0.1	0.3	0.2	0.1	0.1	0.3	0.2	0.4	0.2	0.3	0.1
Cr_2O_3	0.0	0.0	tr.	tr.	0.1	tr.	0.3	0.1	0.0	0.1	tr.	tr.
Al_2O_3	25.8	32.2	20.6	23.8	33.9	35.3	16.3	9.8	12.5	25.3	31.6	32.8
FeO	4.1	2.4	6.3	6.4	0.8	0.2	6.5	9.7	13.3	5.0	3.7	0.7
MnO	0.1	tr.	0.1	0.1	tr.	tr.	0.1	0.1	0.2	0.1	0.1	0.1
MgO	5.7	1.0	7.9	11.6	0.8	tr.	25.6	30.5	24.4	12.0	0.7	0.4
CaO	15.8	17.5	12.2	13.6	19.3	19.4	8.7	6.3	7.1	13.9	17.1	18.4
Na_2O	0.4	0.6	0.4	0.3	0.4	0.3	0.3	0.3	0.2	0.4	0.3	0.5
K_2O	0.1	0.1	0.2	0.1	0.1	0.1	0.1	0.1	0.1	0.1	tr.	0.1
P_2O_5	tr.	tr.	tr.	tr.	tr.	tr.	0.2	0.1	0.1	0.1	tr.	0.2
BaO	tr.	tr.	0.1	0.1	0.1	0.1	0.1	0.1	0.0	0.1	0.1	–
Total	96.0	100.1	99.2	100.5	100.5	98.3	100.8	99.8	99.5	101.3	96.3	98.1
Fo	4.0	0.0	0.0	15.1	0.0	0.0	44.1	50.0	40.5	19.2	0.1	0.0
Fa	2.3	0.0	0.0	6.7	0.0	0.1	8.8	12.8	17.7	6.3	0.5	0.0
En	9.1	2.5	19.8	7.2	2.0	0.0	0.5	4.9	3.5	2.1	1.6	1.0
Fs	4.8	4.4	11.3	2.9	1.3	0.0	0.1	1.2	1.4	0.6	1.1	1.2
Wo	4.3	0.9	2.7	1.6	2.0	1.4	0.0	2.2	0.6	0.7	0.0	1.7
Or	0.7	0.3	0.9	0.6	0.8	0.4	0.5	0.4	0.3	0.8	0.2	0.5
Ab	3.3	5.2	3.3	2.2	3.0	2.6	2.7	2.4	1.8	3.5	2.8	4.0
An	71.3	84.6	54.5	63.3	90.3	94.3	41.9	25.4	33.3	66.0	88.0	89.2
Ilm	0.1	0.1	0.7	0.3	0.2	0.2	0.5	0.4	0.7	0.6	0.2	0.2
Chr	0.0	0.0	0.0	0.0	0.1	0.0	0.4	0.1	0.0	0.2	0.1	0.0
Qtz	0.0	1.8	6.8	0.0	0.3	0.0	0.0	0.0	0.0	0.0	0.0	2.1
Cor	0.0	0.0	0.0	0.0	0.0	0.8	0.3	0.0	0.0	0.0	0.0	0.0
Ap	0.0	0.0	0.1	0.1	0.0	0.1	0.3	0.2	0.2	0.2	0.1	0.0
	1	**2**	**3**	**4**	**5**	**6**	**7**	**8**	**9**	**10**	**11**	**12**

Table 4: Defocused beam analyses of recrystallized (?) intersertal basalt (col. 1), and a granite (col. 2). Column 3 is an estimate of the composition of the Civet Cat norite, from the mode of 60 +/- 10% orthopyroxene and 40 +/- 10% plagioclase, and using two defocused beam microprobe traverses (2mm x 100 microns) in orthopyroxene. and plagioclase-rich areas whose modes were determined.
(from Stoeser *et aI*., in Cl 1, 1974).

SiO_2	47.0	71.2	50.3
TiO_2	0.4	0.1	1.8
Cr_2O_3	0.2	tr.	0.3
Al_2O_3	14.7	12.7	14.4
FeO	15.1	0.6	9.6
MnO	0.3	tr.	0.3
MgO	7.2	0.1	15.7
CaO	13.9	1.1	7.9
Na_2O	0.2	0.2	0.3
K_2O	0.1	8.5	0.1
P_2O_5	0.0	tr.	0.0
BaO	0.1	0.6	–
S	–	–	–
Total	99.2	95.1	100.7
Fo	1.2	0.0	0.0
Fa	2.1	0.0	0.0
En	16.5	0.2	39.0
Fs	25.0	1.0	15.1
Wo	12.7	0.0	0.6
Or	0.6	53.3	0.6
Ab	1.6	1.4	2.5
An	39.3	5.8	37.5
Ilm	0.7	0.2	3.4
Chr	0.3	0.0	0.0
Qtz	–	36.8	1.2
Cor	–	1.3	0.0
Ap	–	0.0	0.0
Troi	–	–	–

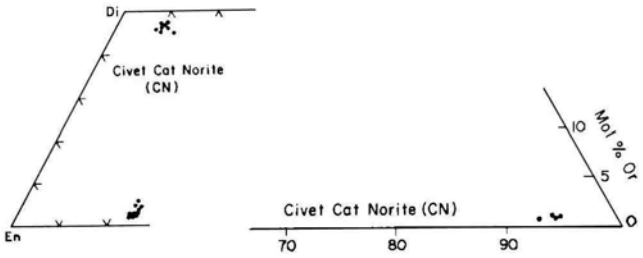

Figure 5: Chemistry of pyroxenes (left) and plagioclases (right) in the 72255 Civet Cat norite. (From Ryder et al., 19756).

metallic iron, and troilite. An exceptional phase is niobian rutile (Marvin, 1975b); two analyses have 19.7% and 18.5% Nb_2O_5, making it the most Nb-rich mineral analyzed (at least by 1975) in any extraterrestrial sample. Ryder et al. (1980a,b) analyzed metal grains in the norite, finding them to be Ni-free, with 2.1 to 4.0% Co. Hansen et al. (1979b) plotted data for an Mg-rich plutonic fragment in 72255 (presumably Civet Cat) on diagrams of Mg' (low-Ca px) v. Ab (plag) and Mg' (liquid, calculated from opx) v. Mg' (plagioclase). (The actual data is not tabulated nor its source described.).

The pyroxenes in the Civet Cat norite were studied by Takeda and his group, to assess the thermal history of the lithology and compare it with eucrites (Takeda and Ishii, 1975; Takeda et al., 1976a,b, 1982; Mori et al., 1980,1982). They used microprobe, x-ray diffraction, and transmission electron microscopy methods. Takeda and Ishii (1975) noted intergranular recrystallization with exsolution of (001) augite from pigeonite well below the pigeonite eutectoid reaction point line; the clinopyroxene inverted to orthopyroxene (Stillwater-type). Takeda et al. (1976a,b) reported microprobe analyses for augite ($En_{46}Wo_{44}$) and orthopyroxene ($En_{73}Wo_2$), and single crystal diffraction results. The pyroxenes showed very weak reflections of secondary pigeonite, as well as minor augite, with pigeonite having (100) in common with host orthopyroxene. The diffraction spots were diffuse because of shock. Augite was detected as lamellae as well as rare small discrete grains. Mori and Takeda (1980) in single crystal diffraction and TEM studies found diffraction patterns for orthopyroxene similar to those in the Ibbenburen eucrite, but also diffraction spots of pigeonite. Mori et al. (1982) and Takeda et al. (1982) reinvestigated the pyroxenes using ATEM for comparison with eucrites and other lunar samples, determining the composition of exsolved augite. The pyroxene differs from that in the 78236 lunar norite in that many grains have abundant augite lamellae (although some have very few). The lamellae average 0.2 microns thick, but are as much as 0.4 microns thick. Opaque inclusions are in the lamellae. The host consists of alternate layers of orthopyroxene and clinobronzite; there are abundant fine clino-bronzite lamellae or stacking faults up to 20 nm present with (100) in common. In some areas wide clinobronzite slabs intrude the orthopyroxene with a comb-like texture. There are no Guinier-Preston zones. Takeda et al. (1982) attribute the presence of the clinobronzite lamellae to shear trans-formation in shock deformation from impact. The exsolution

lamellae are 20x thicker than those in the Johnstown eucrite, and are a product of cooling at depth before shock. The microprobe opx-aug data suggest last equilibration at 900 degrees C, and the ATEM host-lamellae studies suggest 1000 degrees C, suggesting that the latter results from thermal annealing from the shock event. These authors suggested a model-dependent depth of 10 to 70 km for the equilibration.

The apparent primary texture, the wide pyroxene solvus, the narrow compositional ranges, the Ni-free metal, and the bulk and trace element composition (including lack of meteoritic siderophiles) (see below) are consistent with the Civet Cat norite having been a plutonic igneous rock. James (1982) and James and Flohr (1983) classed the Civet Cat norite with the Mgnorites on the basis of its mineralogy and chemistry.

CHEMISTRY

Chemical analyses for the matrix are given in Table 5; for the Civet Cat norite clast in Table 6; and for other materials in Table 7. Rare earth plots for the matrix are shown in Fig. 6, and for the Civet Cat norite and others in Fig. 7.

The average of the matrix analyses is very similar to those of other melt matrices in Boulder 1, including major and trace element chemistry. However, the small samples analyzed by Blanchard et al. (1975, and in Cl 1, Cl 2) show a range, presumably because of unrepresentative sampling (i.e. varied clast contents). (One sample, a subsplit of ,52, is distinct in chemistry, being less aluminous and more ferrous; it is also lighter in color.) Both Blanchard et al. (1975) and Winzer et al. (1975a) emphasize the similarity in composition of 72255 with all other Apollo 17 boulder melts, despite the higher alumina and lower titania of 72255. The k abundance

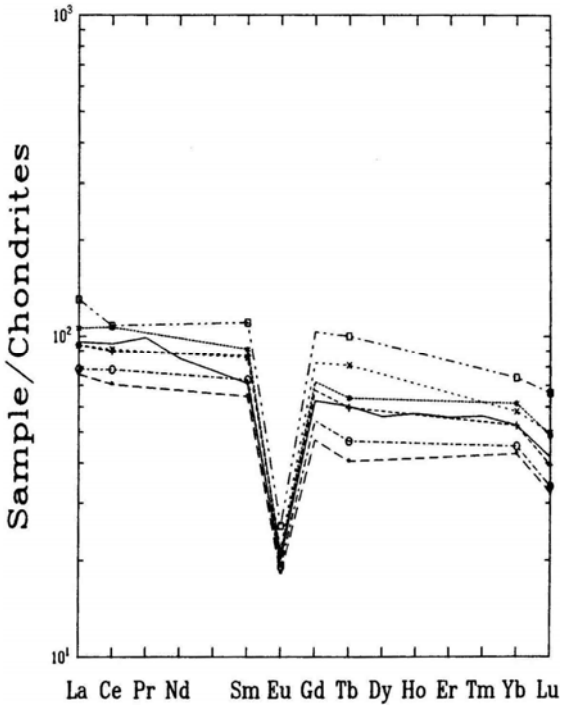

Figure 6: Rare earth element plot for matrix samples of 72255. Solid line without symbols is data of Palme et al. (1978); other data is from Blanchard et al. (1975, and CI 1, C12).

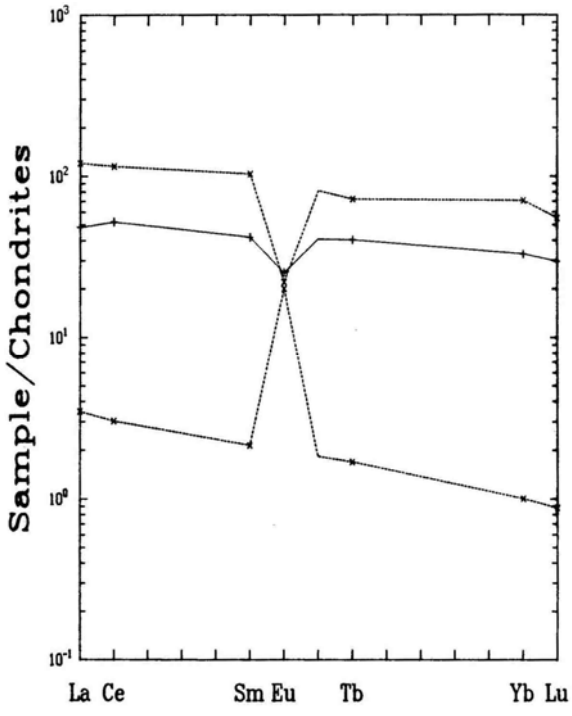

Figure 7: Rare earth element plot for Civet Cat norite (solid line, in center) and the rind (upper dotted line) and core (lower dotted line) of clast #3. All data from Blanchard et al., (1975, and CH, C12).

Table 5: Cbemical analyses of matrix and bulk rock samples of 72255.

	,2		,73(a)	,79(a)	,52(a)	,52(d)	,64(a)	,69(d)	,69(a)	,44	,83	,52	
Split													Split
wt %													wt %
SiO_2			44.8	45.0	49	45.0	45.1	44.7	46	46.72			SiO_2
TiO_2			0.9	0.9	1.4	0.75	0.8	0.8	0.7	0.76			TiO_2
Al_2O_3			19.4	20.7	14.5	20.4	21.9	20.5	19.8	20.82			Al_2O_3
Cr_2O_3			0.630	0.234	0.22	0.232	0.231	0.308	0.46	0.240			Cr_2O_3
FeO			(b)9.05	(c)8.31	14	(d)8.55	(e)7.42	9.5	9.8	8.1			FeO
MnO			0.127	0.129	0.163	0.129	0.12	0.108	0.111	0.117			MnO
MgO			10.5	11.3	9.7	11.3	10.7	10.5	10.4	9.9			MgO
CaO			11.5	12.0	10.7	12.0	12.4	12.3	12.3	12.56			CaO
Na_2O			0.495	0.584	0.32	0.563	0.496	0.400	0.38	0.48			Na_2O
K_2O	0.218	0.221	0.393	0.214	0.27	0.231	0.268	0.280	0.25	0.198			K_2O
P_2O_5										0.252			P_2O_5
ppm													ppm
Sc			15.5	18.2	19.8	18.3	17.3		19.5	18.8			Sc
V													V
Co			2530	28.9	28	25.6	26.6		21	24.5			Co
Ni			7700	260		150	180			150	222	227	Ni
Rb										4.98	6.85	5.8	Rb
Sr										151			Sr
Y										100			Y
Zr										400			Zr
Nb										28			Nb
Hf			9.1	11.2	9.8	10.4	9.9		13.1	10.50			Hf
Ba										328			Ba
Th	4.80	4.4	6.6	5.4		5.8	4.3			4.31			Th
U	1.28	1.20								1.41	1.820	1.790	U
Cs										0.18	0.287	0.240	Cs
Ta				1.5		1.6	1.0			1.27			Ta
Pb													Pb
La			25	31	31	35	26		43	31.7			La
Ce			62	79	80	94	69		95	83.3			Ce
Pr										11.1			Pr
Nd										51			Nd
Sm			11.7	15.7	15.5	16.5	13.2		20	12.86			Sm
Eu			1.26	1.45	1.49	1.44	1.32		1.76	1.39			Eu
Gd										15.6			Gd
Tb			1.9	2.8	3.8	3.0	2.2		4.7	2.83			Tb
Dy										17.7			Dy
Ho										4.00			Ho
Er										11.1			Er
Tm										1.68			Tm
Yb			8.55	10.5	11.6	12.3	9.04		14.8	10.50			Yb
Lu			1.10	1.34	1.69	1.66	1.15		2.25	1.42			Lu
Li										12.8			Li
Be													Be
B													B
C													C
N													N
S										375			S
F										28.0			F
Cl										10.2			Cl
Br										0.03	0.104	0.101	Br
Cu										3.01			Cu
Zn										2.43	2.2	2.8	Zn
ppb													ppb
Au										2.6	2.95	2.00	Au
Ir											7.01	5.28	Ir
I													I
At													At
Ga										3660			Ga
Ge										<100		174	Ge
As										86			As
Se											67	77	Se
Mo													Mo
Tc													Tc
Ru													Ru
Rh													Rh
Pd										<10			Pd
Ag											3.03	0.57	Ag
Cd										<50	6.8	8.1	Cd
In													In
Sn													Sn
Sb											1.74	0.77	Sb
Te											3.3	4.7	Te
W										630			W
Re										0.3	0.503	0.498	Re
Os													Os
Pt													Pt
Hg													Hg
Tl											2.18	1.18	Tl
Bi											0.67	0.21	Bi
	(1)	(2)	(3)	(3)	(3)	(3)	(3)	(3)	(3)	(4)	(5)	(5)	

References and methods:
(1) Fruchter et al (1975); gamma-ray
(2) Keith et al (1974); gamma-ray
(3) Blanchard et al (1975); Cl(1), Cl(2); INAA, AAS
(4) Palme et al (1978); INAA, RNAA, XRP
(5) Morgan et al (1975), Higuchi and Morgan (1975); RNAA C(1).

Table 5: Continued

	,61	,59A(g)	,59B(g)	,59(h)	,53(h)	,53(i)	,67(i)	,54(i)	,60(k)	,52	
Split											Split
wt %											wt %
SiO_2											SiO_2
TiO_2											TiO_2
Al_2O_3											Al_2O_3
Cr_2O_3											Cr_2O_3
FeO											FeO
MnO											MnO
MgO											MgO
CaO										(e)12.0	CaO
Na_2O											Na_2O
K_2O										(e)0.276	K_2O
P_2O_5	0.25										P_2O_5
ppm											ppm
Sc											Sc
V											V
Co											Co
Ni											Ni
Rb		14.95	14.63	9.79	5.69	5.78					Rb
Sr		145.6	141.7	141.2	137.0	141.2				140	Sr
Y											Y
Zr										376	Zr
Nb											Nb
Hf											Hf
Ba										324	Ba
Th							4.222	5.724	6.362		Th
U	1						1.145	1.536	1.663	1.42	U
Cs											Cs
Ta											Ta
Pb							2.478	3.080	3.540		Pb
La											La
Ce											Ce
Pr											Pr
Nd											Nd
Sm											Sm
Eu											Eu
Gd											Gd
Tb											Tb
Dy											Dy
Ho											Ho
Er											Er
Tm											Tm
Yb											Yb
Lu											Lu
Li	11										Li
Be											Be
B											B
C											C
N											N
S											S
F	41										F
Cl	(f)9.1										Cl
Br	(f)0.082										Br
Cu											Cu
Zn											Zn
ppb											ppb
Au											Au
Ir											Ir
I	0.8										I
At											At
Ga											Ga
Ge											Ge
As											As
Se											Se
Mo											Mo
Tc											Tc
Ru	>20										Ru
Rh											Rh
Pd											Pd
Ag											Ag
Cd											Cd
In											In
Sn											Sn
Sb											Sb
Te											Te
W											W
Re											Re
Os	17										Os
Pt											Pt
Hg											Hg
Tl											Tl
Bi											Bi
	(6)	(7)	(7)	(7)	(7)	(7)	(8)	(8)	(8)	(9)	

References and methods:
(6) Jovanovic and Reed (1975 b,c,d, 1980 a); INAA
(7) Compston et al (1975); ID/MS
(8) Nunes et al (1974); ID/MS
(9) Leich et al (1975); irradiation/MS (K, Ca), others ID/MS

Table 5: Continued

Notes:

(a) ,73 Sawdust
,79 Interior Chip
,52 White to light gray matrix
,52 Gray to medium gray matrix
,64 Medium gray material
,69 Dark material
,69 Dark material

(b) INAA; AAS = 9.38%
(c) INAA: AAS = 8.48%

Table 6: Chemical analyes of the Civet Cat norite in 72255.

	,42	,42	,42
Split			
wt %			
SiO_2	52		
TiO_2	0.3		
Al_2O_3	15.5		
Cr_2O_3	0.16		
FeO	7.4		
MnO	0.122		
MgO	15.9		
CaO	9.1		(a) 13.0
Na_2O	0.33		
K_2O	0.08		(a) 0.17
P_2O_5			
ppm			
Sc	13.2		
V			
Co	29		
Ni		4	
Rb		1.27	
Sr			139
Y			
Zr			132
Nb			
Hf	5.5		
Ba			172
Th			
U		0.240	0.45
Cs		0.058	
Ta			
Pb			
La	16		
Ce	46		
Pr			
Nd			
Sm	7.6		
Eu	1.75		
Gd			
Tb	1.9		
Dy			
Ho			
Er			
Tm			
Yb	6.6		
Lu	1.01		
Li			
Be			
B			
C			
N			
S			
F			
Cl			
Br		15.3	
Cu			
Zn		4.5	
ppb			
Au		0.008	
Ir		0.0040	
I			
At			
Ga			
Ge		61	
As			
Se		280	
Mo			
Tc			
Ru			
Rh			
Pd			
Ag		0.76	
Cd		5.8	
In			
Sn			
Sb		0.26	
Te		14.3	
W			
Re		0.0068	
Os			
Pt			
Hg			
Tl		0.30	
Bi		0.30	
	(1)	(2)	(3)

References and methods:
(1) Blanchard et al (1975) and Cl(1), Cl(2); INAA, AAS
(2) Morgan et al (1974, 1975 a, b), Higuchi and Morgan (1975); RNAA, C(1)
(3) Leich et al (1975); irradiation, MS (K, Ca), others ID/MS

Notes:
(a) revised from Cl(2)

Table 7: Chemical analyses of white core and dark rind on clast #3 and other clast material in 72255.

	,45 (a)	,45 (b)	,59 (e)	,53 (f)	,53 (g)
Split					
wt %					
SiO_2	43.0	45.7			
TiO_2	0.65	1.2			
Al_2O_3	35.8	19.7			
Cr_2O_3	0.003	0.263			
FeO	(c) 0.13	(d) 9.05			
MnO	0.003	0.136			
MgO	1.43	11.3			
CaO	18.9	11.5			
Na_2O	0.631	0.542			
K_2O	0.118	0.277			
P_2O_5					
ppm					
Sc	0.45	20.1			
V					
Co	0.33	24.9			
Ni		140			
Rb			1.11	5.52	5.57
Sr			140.6	319.7	190.6
Y					
Zr					
Nb					
Hf	0.10	14.2			
Ba					
Th		6.6			
U					
Cs					
Ta		1.7			
Pb					
La	1.15	40			
Ce	2.68	102			
Pr					
Nd					
Sm	0.39	18.8			
Eu	1.39	1.53			
Gd					
Tb	0.08	3.4			
Dy					
Ho					
Er					
Tm					
Yb	0.202	14.2			
Lu	0.030	1.88			
Li					
Be					
B					
C					
N					
S					
F					
Cl					
Br					
Cu					
Zn					
ppb					
Au					
Ir					
I					
At					
Ga					
Ge					
As					
Se					
Mo					
Tc					
Ru					
Rh					
Pd					
Ag					
Cd					
In					
Sn					
Sb					
Te					
W					
Re					
Os					
Pt					
Hg					
Tl					
Bi					
	(1)	(1)	(2)	(2)	(2)

References and methods:
(1) Blanchard et al (1975; CI 1; CI 2); INAA, AAS
(2) Compston et al (1975, CI 1); ID/MS

Notes:
(a) white
(b) black
(c) INAA
(d) AAS; INAA = 8.77%
(e) anorthosite clast
(f) clear plagioclase
(g) shocked plagioclase

of the bulk rock as measured by gamma-ray is lower than that of the matrix samples (Fruchter et al., 1975). Palme et al. (1978) noted that their analyses of 72255 and 72215 matrix material were similar to some Apollo 16 samples (i.e. 68516) except for the siderophile elements. Higuchi and Morgan (I 975a), Morgan et al. (1975), and Hertogen et al. (1977) assigned the matrix to their siderophile Group 3H (assigned with 72275 to Crisium by Morgan et al., 1974a,b).

The Civet Cat norite (Table 6; Fig. 6) is quartz-normative, and its chemistry is consistent with it being a cumulate plutonic rock containing 20 to 30% of trapped liquid that would be evolved, approaching KREEP (Blanchard et al., 1975). The norite lacks meteoritic siderophile contamination.

Blanchard et al. (1975) analyzed the dark melt rim and the interior white material of clast #3 (45; Table 7, Fig. 7). The rim material is similar to the general matrix; the white material is very anorthositic in major and trace elements, but has a high mg' compared with typical ferroan anorthosites. Rb and Sr analyses for other materials appear to represent varied mixtures of feldspathic material and matrix.

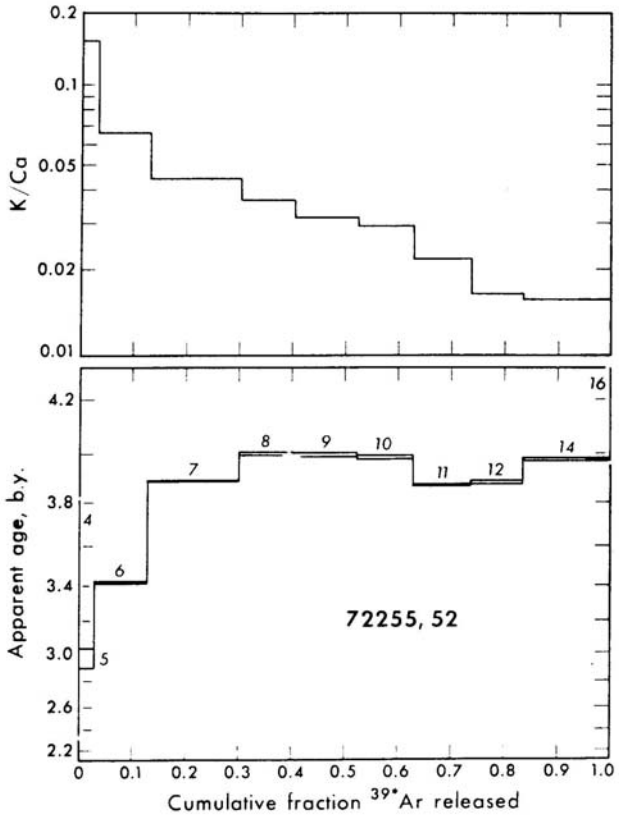

Figure 8: Apparent age and K/Ca data from 72255,52 matrix (Leich et al., 1975a). The ages shown correspond with the "old" decay constant; recalculation shows that the two highest plateaus correspond with 3.93 Ga, and steps 11 and 12 with about 3.83 Ga.

RADIOGENIC ISOTOPES AND FISSION TRACK AGES

Schaeffer *et al.* (1982a,b) used laser Ar-Ar techniques to determine ages of clasts and to infer the age of the melt in section 72255,134, providing 20 analyses (Table 8). Most of the ages were for plagioclase or plagioclase-composite clasts; two were for felsite ("feldsparthoid") clasts. The two felsites, the most K-rich fragments, give ages generally younger than the feldspars. The higher ages for the plagioclases, some of which are in noiitic lithic clasts, range up to 4.29 Ga. Schaeffer *et al.* (1982a b) suggest that the age of the felsite clasts, which probably degassed during melting, is the best estimate for the age of the melt groundmass, which is therefore about 3.85 Ga, the age of the most precisely dated of the felsites. (The felsite clasts were preheated to 650 degrees C; the ages are total release, hence K-Ar, of the greater than 650 degrees C fraction. Assuming a well-developed plateau above that temperature, the ages are reliable).

Leich *et al* (1975a) reported Ar-Ar analyses for a matrix sample of 72255 (Fig. 8). Leich et al. (1975a) believe that the intermediate-temperature (800 to 1000 degrees C) and the high-temperature (1400 degrees C) plateaus are reliable indicators of the age of the sample; these plateaus give an age of 3.93 Ga. However, the age of the 1000 to 1400 degree release is the one that agrees with the age inferred by Schaeffer *et al.* (1982a,b), and the Leich et al. (1975a) plateaus must be compromised by the plagioclase clasts that did not completely degas.

Compston *et al.* (1975) reported Rb-Sr isotopic data for matrix and small clast samples of 72255 (Table 9). For split ,53 the total rock and plagioclase clasts are well-aligned on a 4.30 +/- 0.24 Ga "isochron" which should be regarded as a mixing line rather than a true isochron (Fig. 9). The clasts are not cogenetic, and the data for 72215 shows that the clasts and matrix did not reach Sr isotopic equilibration, and so 4.30 Ga does not date the assembly of the breccia. Split,59 materials also fall on a mixing line that is the chance result of mixing unrelated anoithositic material, unidentified old "basaltic" material (i.e. low-K Fra Mauro source

Table 8: Laser microprobe data for materials in 72215,144.
Recalculated from Schaeffer *et al*., 1982a, b).

Phase	K%	Ca%	Ar40/39		Age Ga	
Plag	0.02	8	37.31+/- 0.333.917 +/-.027			
Plag	0.02	3.4	38.56	1.73	3.970	.076
Plag	0.04	8	33.60	1.28	3.753	.065
Plag	0.02	3.5	36.25	1.73	3.872	.079
Plag-comp	0.09	3.6	47.04	0.62	4.288	.032
Plag-comp*	0.30	<10	43.43	0.99	4.161	.050
Plag-comp	0.05	1.3	43.96	1.00	4.179	.044
Plag-comp*	0.04	<10	37.92	1.42	3.924	.069
Plag-comp	0.04	3	38.72	0.61	3.976	.034
Plag-comp*	0.04	<10	40.07	10.00	4.082	.350
Plag	0.19	15	36.31	0.50	3.874	.032
Plag	0.05	4	40.70	1.52	4.055	.065
Plag-comp	0.12	3	38.85	0.31	3.981	.026
Plag-comp*	0.16	<10	36.02	1.24	3.912	.065
Plag	0.02	3	33.36	0.73	3.740	.041
Matrix	0.10	4	37.02	0.35	3.905	.027
Matrix	0.27	5	34.07	0.19	3.774	.024
Matrix	0.32	12	37.60	0.32	3.929	.027
Felsite*	3.9	<10	34.63	0.57	3.846	.043
Felsite*	2.3	<10	32.75	2.75	3.767	.135

(Samples degassed at 225 degrees centigrade during bakeout after sample loading).
* = preheated at 650 degrees centigrade

Table 9: Rb-Sr isotopic data for samples from 72255
(Compston *et al.*, 1975)

Sample	Mass mg	Rb ppm	Sr ppm	87Rb/86Sr	87Sr/86Sr +/-se
,59 gray A	16.2	14.95	145.6	0.2967	0.71693+/-6
,59 gray B	16.8	14.63	141.7	0.2983	0.71695 4
,59 light gray	19.7	9.79	141.2	0.2001	0.71116 4
,59 anorth clast	4.3	1.11	140.6	0.02275	0.70050 8
,53 lt-gy1	29.0	5.69	137.0	0.1198	0.70664 6
,53 lt-gy2	14.0	5.78	141.2	0.1183	0.70642 3
,53 plag 1 (clear)	0.8	5.52	319.7	0.0499	0.70223 11
,53 plag 2 (shocked)	3.1	5.75	190.6	0.0871	0.70450 8

se = internal standard error of mean
,59 gray = plagioclase clasts in opaque matrix
,59 lt gy = plagioclase clasts smaller, subrounded, matrix texture variable
,53 lt gy = coherent uniform matrix with angular plagioclase and small anorthosite clasts
A,B = duplicates from reasonably homogeneous powder

Table 10: Concentrations of U, Th, and Pb in 72255 samples.
(Nunes *et al.*, 1974b)

Sample	Weight (mg)	Concentrations (ppm) U	Th	Pb	$^{232}Th/^{238}U$	$^{238}U/^{204}Pb$
72255,67 matrix (dark)	132.5	1.145	4.222	2.478	3.81	1,414
72255,54 matrix (light)	98.2	1.536	5.724	3.080	3.85	2,998
72255,60 matrix mixture (dark and light)	196.7	1.663	6.362	3.540	3.95	2,135
72255,49 Civet Cat clast plag.-deficient	51.6	0.3874	1.216	0.9448	3.24	195
72255,49 Civet Cat clast plag.-enriched	35.7	0.2151	—	0.6939	—	177

*Concentration run divided from solution; all other analyses were of splits from crushed solid material obtained prior to spiking.

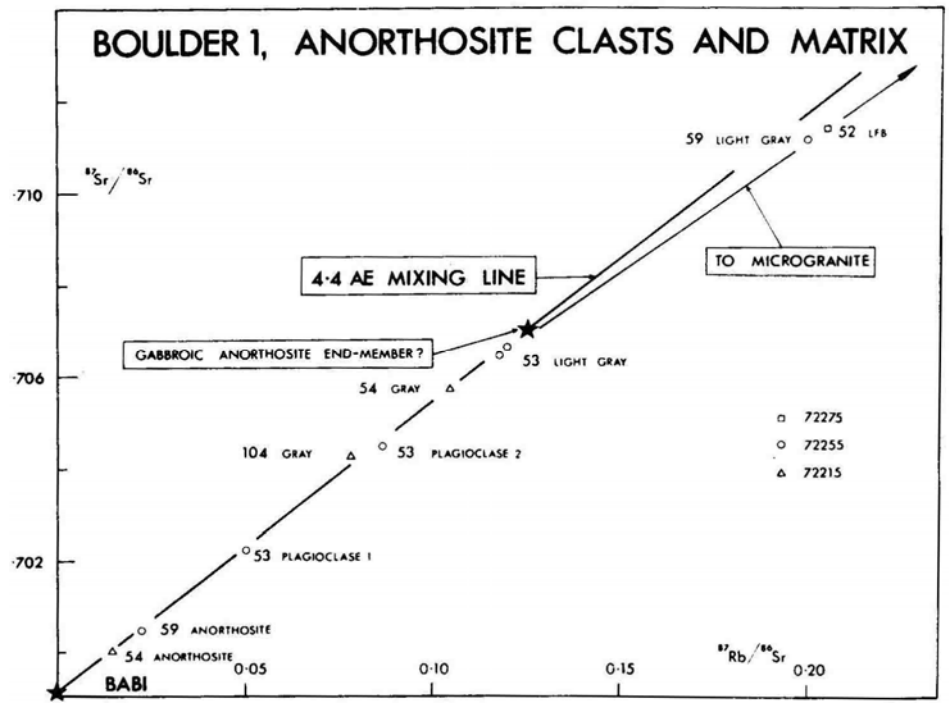

Figure 9: Mixing lines generated by anorthositic clasts within breccia matrix samples and an unidentified gabbroic anorthosite end-member; and between gabbroic anorthosite and microgranite, for 72255 and other Boulder I samples. If anorthositic samples are cogenetic, the line marked 4.4 Ae defines their igneous age. Using new decay constants, this line has an age of 4.31 Ga. (See also 72215, Fig. 9).

Table 11: Isotopic composition of Pb in 72255 samples.
(Nunes *et aL*,1974b)

Sample	Run	Corrected for blank and primordial Pb				Single-stage ages in m.y.			
		$\frac{^{206}Pb}{^{238}U}$	$\frac{^{207}Pb}{^{235}U}$	$\frac{^{207}Pb}{^{206}Pb}$	$\frac{^{208}Pb}{^{232}Th}$	$\frac{^{206}Pb}{^{238}U}$	$\frac{^{207}Pb}{^{235}U}$	$\frac{^{207}Pb}{^{206}Pb}$	$\frac{^{208}Pb}{^{232}Th}$
72255,67 matrix (dark)	C1P	0.9906	77.36	0.5667	0.2459	4,480	4,486	4,489	4,503
	C1	0.9873	77.22	0.5676	—	4,469	4,484	4,491	—
72255,54 matrix (light)	C1P	0.9321	66.41	0.5170	0.2324	4,285	4,331	4,353	4,281
	C1	0.9317	66.13	0.5151	—	4,284	4,327	4,348	—
72255,60 matrix mixture (dark and light)	C1P	0.9745	74.53	0.5550	0.2349	4,427	4,448	4,458	4,322
	C1	0.9743	74.61	0.5557	—	4,426	4,449	4,460	—
72255,49 Civet Cat clast plag.-deficient	C1P	1.065	92.15	0.6281	0.2499	4,717	4,664	4,641	4,570
	C1	1.069	90.76	0.6159	—	4,732	4,649	4,612	—
72255,49 Civet Cat clast plag.-enriched†	C1P	1.464	147.8	0.7326	—	5,382	5,050	4,916	—
	C1	1.443	169.7	0.8533	—	5,867	5,146	4,865	—

*Note: Concentration and composition splits were divided from solution prior to adding the ^{208}Pb enriched spike. All other analyses were of splits from crushed solid material and the concentration portions were totally spiked prior to dissolution.

†The gross difference between the CP and C only calculations must be because of an heterogeneous splitting of this sample prior to spiking—calculated U/Pb ratios from the concentration only data (i.e. where only the $^{208}Pb/^{206}Pb$ ratio from the composition run was utilized) are the most accurate.

Table 12: Age parameters and single-stage Pb ages of 72255 samples.
(Nunes et al., 1974b).

Sample	Weight (mg)	Run	Observed ratios†			Corrected for analytical blank‡				
			$\frac{^{206}Pb}{^{204}Pb}$	$\frac{^{207}Pb}{^{204}Pb}$	$\frac{^{208}Pb}{^{204}Pb}$	$\frac{^{206}Pb}{^{204}Pb}$	$\frac{^{207}Pb}{^{207}Pb}$	$\frac{^{208}Pb}{^{204}Pb}$	$\frac{^{207}Pb}{^{206}Pb}$	$\frac{^{208}Pb}{^{206}Pb}$
72255,67 matrix (dark)	100.8	P	1,596	908.5	1,526	2,815	1,601	2,682	0.5685	0.9527
	132.5	C*	1,092	624.7	—	1,405	802.5	—	0.5711	—
72255,54 matrix (light)	124.1	P	2,089	1,085	2,023	3,296	1,709	3,186	0.5187	0.9666
	98.2	C*	1,734	898.9	—	2,803	1,449	—	0.5171	—
72255,60 matrix mixture (dark and light)	190.3	P	1,987	1,107	1,909	2,212	1,233	2,128	0.5573	0.9619
	196.7	C*	1,897	1,060	—	2,090	1,166	—	0.5582	—
72255,49 Civet Cat clast plag.-deficient	66.2	P	185.7	120.9	163.5	198.2	128.9	173.3	0.6505	0.8743
	51.6	C*	199.2	127.2	—	217.6	138.6	—	0.6369	—
72255,49 Civet Cat clast plag.- enriched	32.9	P	204.9	153.2	148.8	245.4	183.3	173.3	0.7467	0.7062
	35.7	C*	160.0	138.5	—	180.5	156.4	—	0.8663	—

*Samples totally spiked prior to digestion.

†^{208}Pb spike contribution subtracted from Pb concentration data.

‡Analytical total Pb blanks ranged from 0.59 to 1.96 ng except for the 75055 composition blank (2.9 ng), and the 74220 concentration blank (2.8 ng).

P = composition data; C = concentration data.

Table 13: Fission track analysis of whitlockite in 72255

(from Goswami et al., 1976a). Track density in cm-2 x 107. The table differs from that in Goswami and Hutcbeon (1975) in that the observed track density has increased from 30.2 and the row labelled "spallation recoils" has been added, exactly accounting for the increase. Goswami and Hutcheon (1975) also mislabelled the density units as being multiplied by a factor of 10-7 instead of 107.

Track contributions	72255*
Observed track density	36.3 ± 1.5
Fe-group cosmic rays	1.0 ± 0.5
Spallation recoils	6.1 ± 0.6
Reactor-induced fission	1.65 ± 0.06
Lunar neutron-induced fission	< 0.15
High-energy cosmic ray-induced fission‡	$3.3^{+1.7}_{-1.0}$
Spontaneous fission tracks	$24.2^{+1.7}_{-2.2}$
Tracks from ^{238}U fission	16.1 ± 1.1§
Tracks from ^{244}Pu fission	$8.1^{+1.8}_{-2.4}$§
Observed ρ_{Pu}/ρ_U	$0.51^{+0.10}_{-0.14}$

*Goswami and Hutcheon (1975).
†This work.
‡Assumes Th/U = 12*‡.
§C_a = 71 ± 4 ppm; track retention age = 3.96 G.y.
¶C_a = 83 ± 4 ppm; track retention age = 3.98 G.y.
Calculations use the following decay constants: $\lambda_F^{238} = 7.03 \times 10^{-17}$ yr^{-1} (Roberts *et al.*, 1968); $\lambda_D^{238} = 1.55 \times 10^{-10}$ yr^{-1} (Jaffey *et al.*, 1971); $\lambda_F^{244} = 1.045 \times 10^{-11}$ yr^{-1} (Fields *et al.*, 1966); $\lambda_D^{244} = 8.50 \times 10^{-9}$ yr^{-1} (Fields *et al.*, 1966).

Table 14: Rb-Sr data for the Civet Cat norite in 72255

(Compston *et al.*, 1975).

Rb, Sr, and $^{B7}Sr/^{86}Sr$ for samples of the Civet Cat clast 72255,41. Total-rock samples are independent fragments rather than homogenized aliquots, so analytical differences are expected due to sampling effects. Mineral separates are grouped with the total-rocks from which they were separated

	Weight (mg)	Rb (ppm)	Sr (ppm)	$^{87}Rb/^{86}Sr$	$^{87}Sr/^{86}Sr \pm se$[a]
Plagioclase-rich total-rock (1)	5.2	4.20	219.5	0.0552	0.70250 ± 7
Plagioclase-rich total-rock (2)	4.3	3.96	226.5	0.0504	0.70222 ± 3
'Mixed' total-rock (1)	15.8	2.56	101.4	0.0729	0.70348 ± 2
'Mixed' total-rock (2)	14.6	3.02	100.9	0.0864	0.70443 ± 2
Plagioclase (1)	4.5	3.59	224.6	0.0461	0.70203 ± 3
Plagioclase (2)	4.6	3.60	221.2	0.0469	0.70202 ± 3
Plagioclase (3)	3.6	3.29	209.5	0.0453	(0.70168 ± 8)[b]
Plagioclase (4)	3.7	2.89	198.0	0.0421	0.70175 ± 3
Pyroxene (green)	8.8	1.09	16.12	0.1956	0.71080 ± 15
Pyroxene (black)	3.7	0.74	22.08	0.0972	0.70518 ± 6
Pyroxene-rich total-rock (1)	15.5	5.68	79.8	0.2053	0.71148 ± 3
Pyroxene-rich total-rock (2)	14.4	5.75	99.7	0.1662	0.70919 ± 4
Plagioclase (5)	5.6	6.67	147.1	0.1309	0.70743 ± 3
Pyroxene (green+black)	4.3	1.80	19.16	0.2721	0.71498 ± 8

[a] Internal standard error of mean.
[b] Strong anomalous isotopic fractionation – discard.

material), and granitic material (see 72215, Fig. 9 for diagram). U,Th-Pb isotopic data and age parameters for matrix samples were presented by Nunes et at (1974b) (given here as Tables 10, 11, and 12, with data for the Civet Cat norite), and also discussed by Nunes and Tatsumoto (1975). The matrix data plot within error of concordia in a 4.24 to 4.44 Ga range (see 72215, Fig. 10). Although these Boulder 1 data can by themselves be explained by a simple 2-stage U-Pb evolutionary history whereby ~4.5 Ga material was disturbed by ~4.0 Ga event(s), other intermediate events could be masked by the uncertainty of the data Hutcheon et al. (1974b), Braddy et at (1975b), Goswami and Hutcheon (1975), and Goswami et at (1976a,b) used fission tracks to assess the age of a whitlockite grain in the 72255 matrix (Table 13, Fig. 13). Adopting 71 ppm U for the whitlockite, the tracks are in excess of those from ^{238}U alone, and the excess is assumed to result from ^{244}Pu. A (Pu/[no of 0.020 gives an age of 3.90-3.93 Ga for the whitlockite (Hutcheon et al., 1974b); if the ratio is assumed to be the same as that of the St. Severin meteorite, i.e. 0.015, then the age is 3.96 (+0.04,- 0.07) Ga. Such a track retention age of the whitlockite most probably refers to the last high-temperature event.

Radiogenic isotopes in the Civet Cat norite clast were investigated by Leith et al. (1975a,b) (Ar-Ar), Compston et al. (1975) (Rb-Sr), and Nunes et at (1974b) and Nunes and Tatsumoto (1975a) (U,Th-Pb). The Ar-Ar release data are shown in Fig. 10. From 800 to 1200 degrees Centigrade the sample has an apparent-age plateau of 3.93 +/- 0.03 Ga; the plateau includes 57% of the total ^{39}*Ar. The 1400 degree centigrade fraction has an age significantly higher (~3.99 Ga) and contains 25% of the total ^{39}*Ar. The Ar isotopic data as a whole suggest that the plateau age is reliable, and it is consistent with the disturbances indicated in the Sr

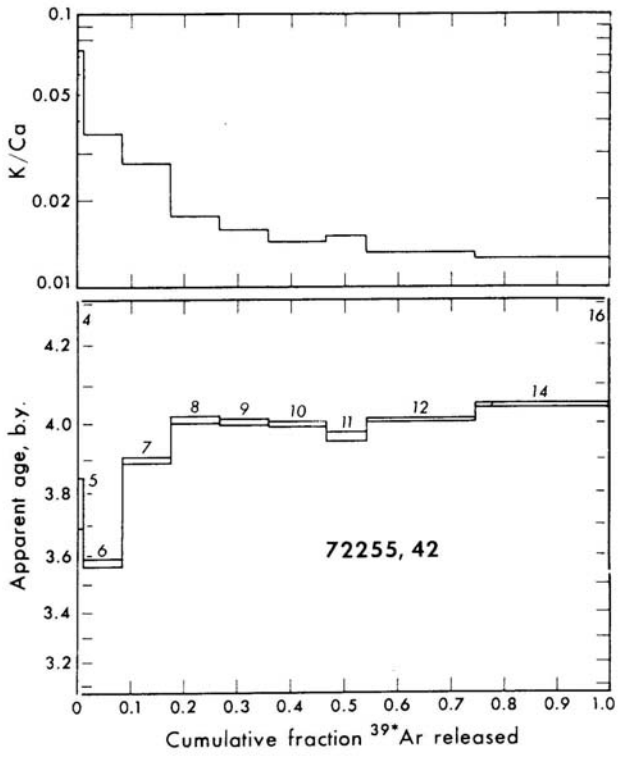

Figure 10. Apparent-age and K/Ca data from 72255,42. (Leith et al., 1975a)

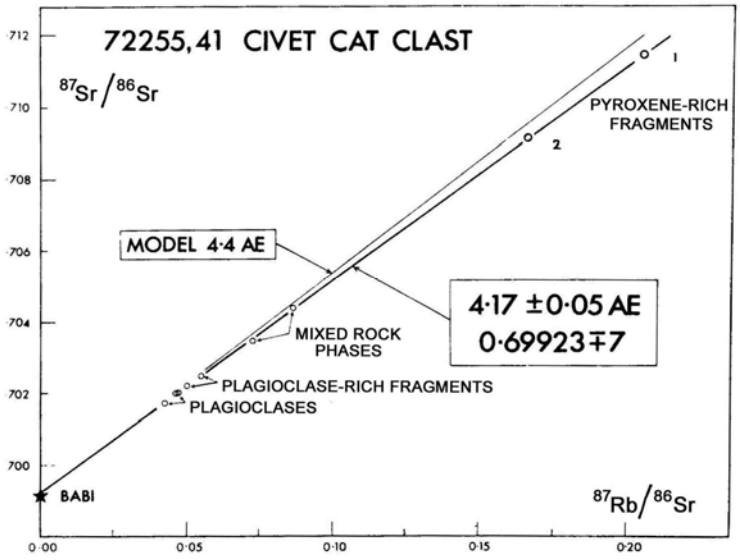

Figure 11: Isochron defined by total-rock fragments and low-Rb plagioclases from the Civet Cat clast (72255,41). The age with new constants is 4.08 Ga: the model line corresponds with 4.31 Ga (Compston et at, 1975)

and Pb isotopic data. The Rb-Sr isotopic data for the Civet Cat are given in Table 14, and Figs. 11, 12, and 13, and include many mineral separates. The six "bulk" samples alone define a perfectly fitted isochron of 4.10 +/- 0.06 Ga, with initial $^{87}Sr/^{86}Sr$ of 0.69919 +/- 8 (Fig. 11). Compston *et al.* (1975) interpret this age as the igneous crystallization age, because (1) these entitities were created during an igneous event (2) the intitial Sr isotope ratio is low whereas the Rb/Sr is quite high, and (3) metamorphic equilibration in the sample is limited to smaller volumes. Including the plagioclase separates refines the age to 4.08 Ga. Some separates do not fit the "bulk" isochron (Fig. 12), and the pattern resembles that of response to a younger heating event; however, re-equilibration was not complete on the scale of less than 0.2 mm. An age of 3.81 +/- 0.23 Ga approximates the time of mineral disturbance. A detailed discussion is given in Compston *et al.* (1975). Alternatively, if the Civet Cat was not a closed system during re-heating, then those separates richest in Rb might represent Rb gain. Then an alignment of black pyroxene, plagioclase-rich total rocks, and other plagioclases give an age of about 4.36 +/- 0.13 for the maximum possible original crystallization age.

The U,Tb-Pb isotopic data of Nunes *et al.* (1974b) for the Civet Cat norite are in Table 10. The Civet Cat norite contains excess Pb relative to U, plotting well above concordia. The excess probably reflects transfer of Ph from the matrix, which is relatively Pb-rich, into the clast during breccia formation, although other times are possible. The two analyses are too uncertain to yield an accurate age determination (Nunes and Tasumoto, 1975a).

EXPOSURE AGES:

Leich *et al.* (1975a,b) measured the isotopic compositions of the rare gases He, Ne, Ar, Kr, and Xe in a matrix sample and the Civet Cat norite in 72255. Trapped gas abundances are very low, with only small to negligible solar wind components. The cosmogenic Kr isotopic spectra for the matrix sample gave an exposure age of 44.1 +/- 3.3 Ma. (Leich *et al.,* 1975b, tabulated preliminary Kr ages of 44.6 +/- 2.9 for the matrix and 36 +/-10 for the Civet Cat, but in Leich *et al.,* 1975a, no Kr age was tabulated for the Civet Cat norite sample because there are large uncertainties in the cosmo-genic $^{81}Kr/^{83}Kr$ ratio). The age is similar to that of 72215, but lower than the exposure age of 72275 (52 Ma), probably because of differences in shielding. The less-precise Ar-Ca exposure ages (48 Ma for Civet Cat, 56 Ma for matrix, +/-about 25%*)* are consistent with the Kr age.

Particle track data bearing on exposure were reported by MacDougall *et al.* (1974), Hutcheon *et al.* (1974b), Braddy *et al.* (1975b), Goswami and Hutcheon (1975), and Goswami *et* al. (1976a,b). The track density profile was produced from thick sections 72255,30 and ,32, using SEM and optical methods. The interpretation is complicated by correction for exposure geometry (assumed equivalent to present-day exposure throughout) and uncertainty in the erosive history (assumed as 1 mm/Ma). The external surface of the sample is saturated with craters, suggesting a recent exposure of more than 1 Ma. Hutcheon *et al.* (1974b) using a simple one-stage exposure model calculated an age of 19 +/-2 Ma. The uneven distribution of shock alteration effects could be a complicating factor. Goswami and Hutcheon (1975) added more data (Fig. 14); they found that if normalized to the Kr exposure age of 42 Ma, then agreement at depths greater than 1 cm was good, but not at less than this depth (Fig. 15). The disagreement could result from small-scale (mm size) cratering event late in the boulder history. MacDougall et al. (1974) had placed an upper limit of 15 to 20 Ma on the exposure, but noted that erosion was in any case a problem for interpretation; such track ages do not necessarily date the time that the boulder rolled into its present position, but only some later spalling event.

Yokoyama et al. (1974) noted that 72255 was saturated in ^{26}Al, requiring an exposure of at least a few million years.

PHYSICAL PROPERTIES

Magnetic data for 72255 samples were reported by Banerjee *et al.* (1974a,b) and Banerjee and Swits (1975). Samples from the Boulder were oriented with respect to each other (accurate to within about +/- 20 degrees). Two samples from 72255 had the same direction (Fig. 16), and within error of those from 72255. The two 72255 samples had the same intensity of 1.2×10^{-5} emu/g. In an attempt to separate stable primary NRM from unstable secondary NRM, the authors attempted thermal demagnetization, avoiding oxidation; however, from the continually decreasing NRM (Fig. 17), it appeared that perm-anent damage was done to the magnetic carriers and the procedure was unadvisable. AF-demagnet-ization showed no zig-zag patterns, and the NRM direction after demagnetization in fields at 80 Oe or greater are stable and primary; however, these fields differ in direction from those in 72275 by 130 degrees (Fig. 18). Banerjee and Swits (1975) presented data for paleointensity, suggesting a field of 0.35 Oe, different from those of 72275 and 72215 (suggesting 3 different events, as also suggested by the differing directions of NRM under AF demagnetization). However, given the problems of

obtaining and interpreting magnetic data for lunar samples then neither the directions nor the intensities can be said to have known meanings (see also discussion by Cisowski et al., 1977).

Adams and Charette (1975) reported spectral reflectance measurements for the 0.35-2.5 micron range for a gray noritic breccia that was heavily contaminated with saw-blade metal (,74). The reflectance curve may be artificially flattened by the presence of the opaque contaminant; it shows little absorption at the 1.9 micron band that results from pyroxene and that is typical of other highland rock samples.

PROCESSING

The details of the intial processing of 72255 were given by Marvin in CI 1 (1974). Three documented pieces had broken away during transport, and partly used for thin sections. The sawing of a 1.5 cm_ thick slab (Figs. 1,2) was accomplished in July, 1973. The slab, 72255,10, was removed as a single piece and, I 1 broke off along a pre-existing crack. Some chalky white material was sawn from the east tip (,18) and used for thin sections and chemistry, and surface chips were taken from elsewhere on the main mass (Fig. 2). The slab was subdivided, with the maul divisions as shown in Fig. 19. Many thin sections were made from slab materials. A second slab and related pieces were cut from the main mass 72255,23 in 1984, but studies of them have only recently commenced.

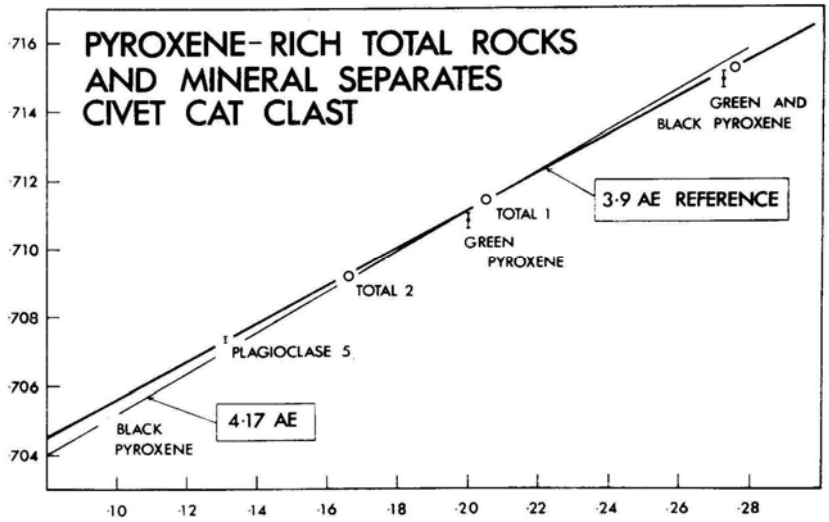

Figure 12: Rb-Sr mineral data for the pyroxene-rich fragments of the Civet Cat class. With new constants, the "3.9 Ga reference line" corresponds with 3.82 Ga reference, and the 4.17 isochron to 4.08 Ga. The reference isochron corresponds with the time of redistribution of ^{87}Sr and/or Rb after original igneous cooling at 4.08 Ga. (Compston et al., 1975).

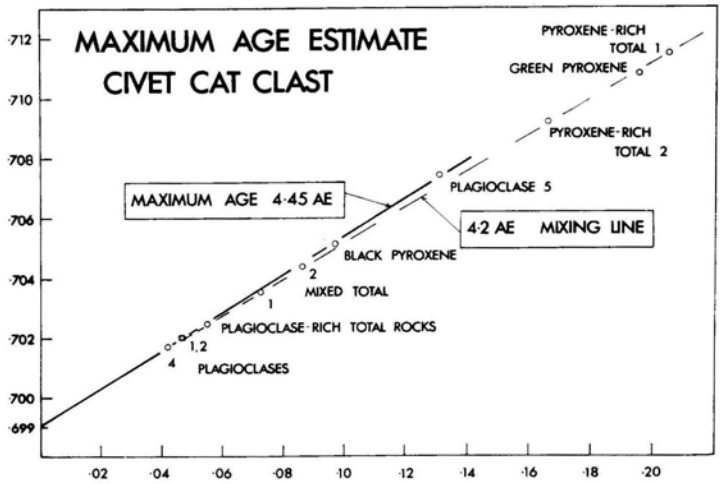

Figure 13: Maximum age estimate for the Civet Cat norite (4.36 Ga with new decay constants). The diagram assumes that new Rb entered the pyroxene-rich component during deformation and shearing at breccia assembly, but that all plagioclase separates and black pyroxene were unaffected. Then the "4.2" Ga (new constants give 4.11 Ga) becomes a mixing line of no simple time significance. (Compston et al., 1975).

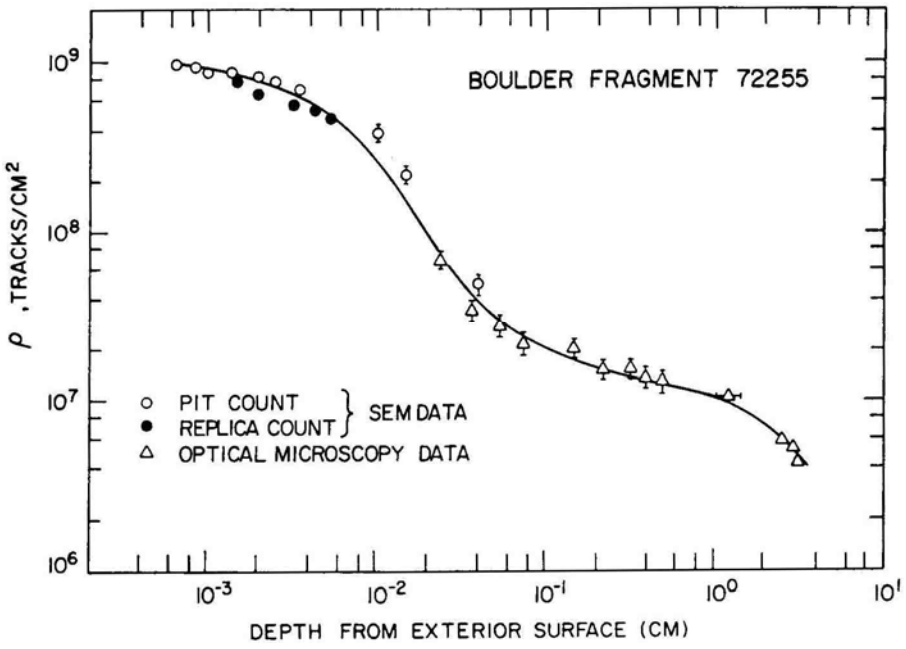

Figure 14: Measured track densities in 72255,30 and,32 plotted as a function of distance from the exterior surface. SEM and optical data, without normalization. The solid line is the best fit through the data points. (Goswami and Hutcheon, 1975).

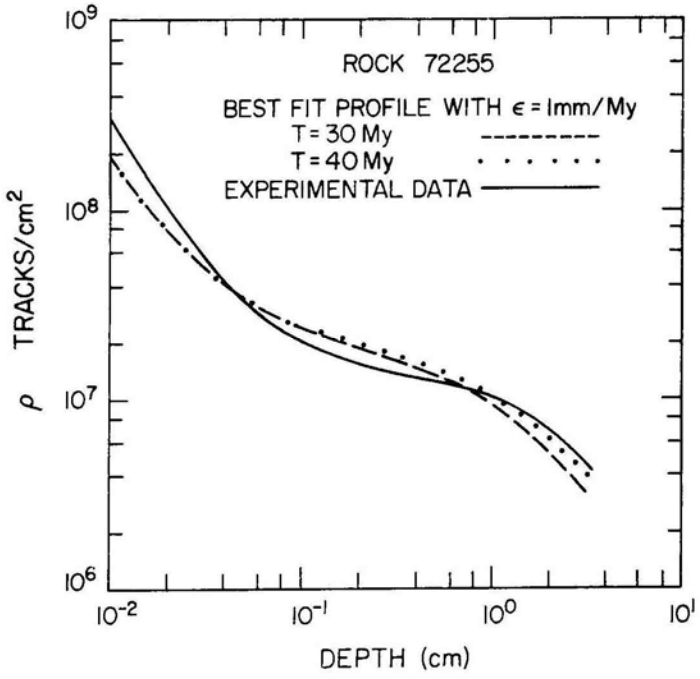

Figure 15: Observed and expected track density profiles for 72255. The solid line is taken from Figure 14, the dotted and dashed lines are calculated for two different exposure ages. (Goswami and Hutcheon, 1975).

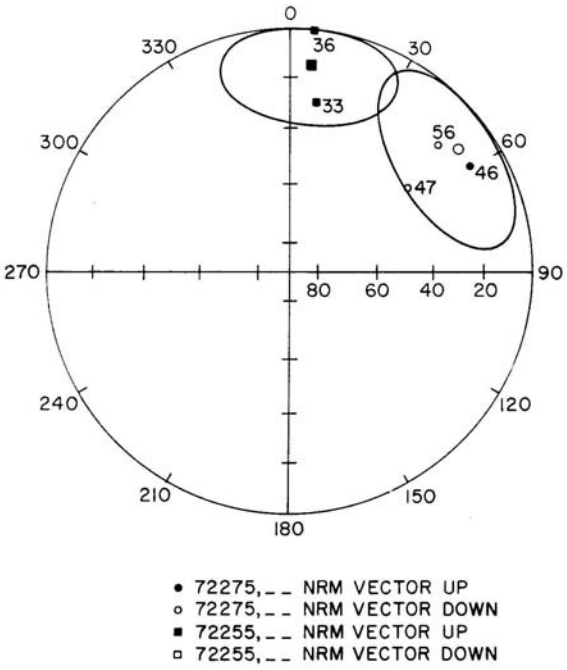

Figure 16: Absolute NRM directions of samples of 72255 and 72275. Average directions for each sample are denoted by the larger symbols. 95% cones of confidence are indicated. (Banerjee et al., 1974a).

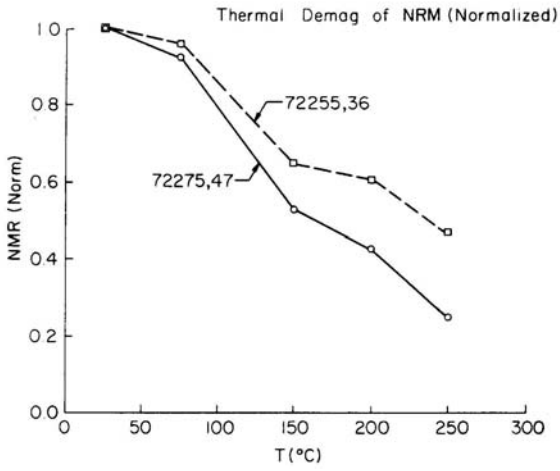

Figure 17: Decay of NRM intensity on thermal demagnetization of 72255 and 72275 samples in zero field and in an H_2-CO_2 gas-buffered furnace. (Banerjee et al., 1974x).

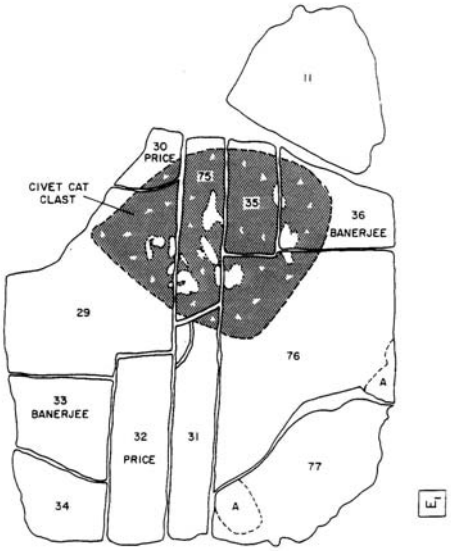

Figure 18: Main subdivisions of the first slab cut from 72255, in 1973 (from Marvin, in CI 1, 1974).

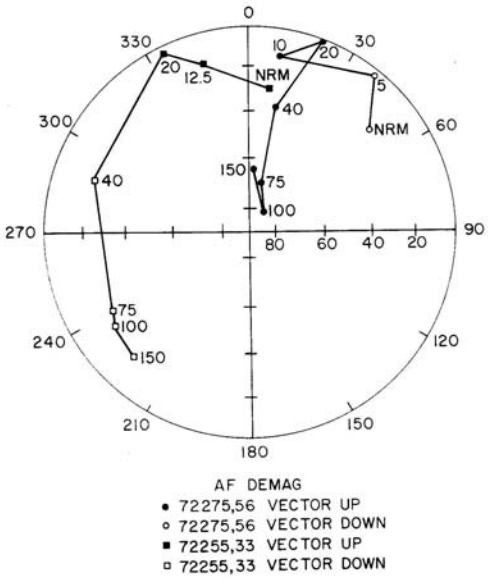

Figure 19: Changes in NRM directions on AF-demagnetization of 72255 and 72275 samples. The numbers refer to peak AF values. The stable direction for 72275 is average of points 75,100, and 150; that for 72255 for points 75 and 100. (Banerjee et al, 1974a).